Solar Powered E-Bike Charging Station with AC, DC and Contactless Charging

Chandra Mouli, Gautham Ram; van Duijsen, Peter; Velzeboer, Tim; Ganesan Nair, Gireesh; Zhao, Yunpeng ; Isabella, Olindo; Bauer, Pavol; Jamodkar, Ajay; Silvester, Sacha; Zeman, Miro

Publication date
2018

Document Version
Accepted author manuscript

Published in
2018 20th European Conference on Power Electronics and Applications (EPE'18 ECCE Europe)

Solar powered e-bike charging station with AC, DC and contactless charging

Gautham Ram Chandra Mouli, Peter van Duijsen, Tim Velzeboer, Gireesh Nair, Yunpeng Zhao, Ajay Jamodkar, Olindo Isabella, Sacha Silvester, Pavol Bauer, Miro Zeman
Delft University of Technology
Department of Electrical Sustainable Energy, Building 36, Mekelweg 4
2628CD Delft, The Netherlands
Tel.: +31 15 27 84654
E-Mail: P.Bauer@tudelft.nl
URL: http://www.tudelft.nl

Acknowledgements

The authors would like to acknowledge the support of Harrie Olsthoorn, Joris Koeners, Bart Roodenburg of the DC systems, Energy conversion and Storage group of the Delft University of Technology, the Netherlands. We thank Delft Infrastructure & Mobility Initiative, 3E fonds and Climate-KIC and Involar for their support of this project.

Keywords

Battery charger, Contactless Energy Transfer, Electric vehicle, Photovoltaic, Power converter for EV

Abstract

Charging electric vehicles from solar energy provides a sustainable means of transportation. This paper shows the design of solar powered e-bike charging station that provides AC, DC and contactless charging of e-bikes. The DC charger allows direct DC charging of the e-bike from the DC power of the photovoltaic panels (PV) without the need for an external AC charger adapter. In case of the contactless charger, the bike can be charged without the use of any cables providing maximum convenience to the user. Finally, the charging station has an integrated battery that allows for both grid-connected and off-grid operation.

Introduction

Electric vehicles (EVs) like electric cars, e-bikes or trucks provide a clean and pollution-free mode of transportation. However, electric vehicles are only sustainable if the electricity used to charge them comes from sustainable sources of energy. The current electricity grid is still primarily powered by

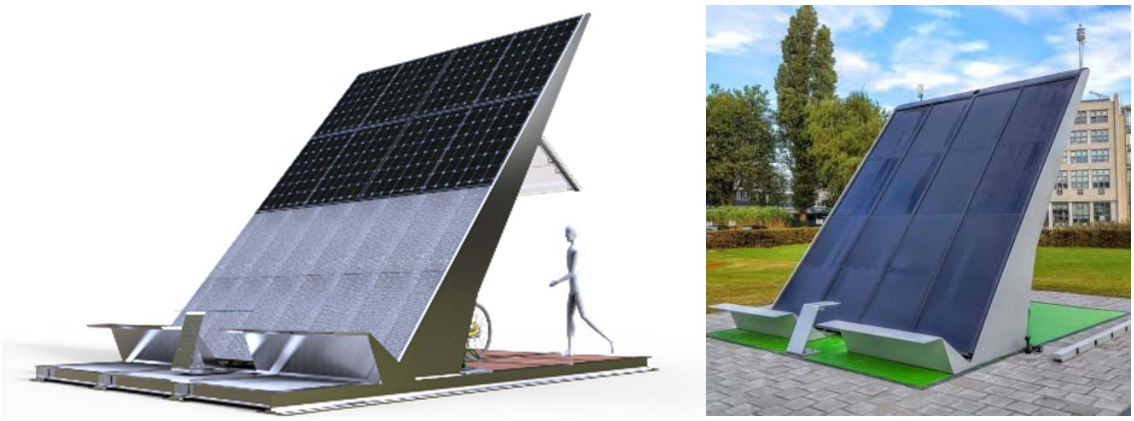

Fig. 1. Artistic impression of solar e-bike charging station (left) and realization in university campus (right)

fossil fuels. Hence, EVs charged from such a grid results in indirect emissions at the power plant [1], [2]. Therefore, electric vehicles are only sustainable when charged from sustainable sources of electricity like solar and wind [1]–[5].

Workplace charging of electric vehicles from photovoltaic panels has a significant potential for the future. The solar panels can be installed on office buildings or at the parking lot, a potential, mostly untapped today. A few of the noteworthy benefits of charging EV from PV are:

1. EVs can be charged at the workplace during the day, at the same time PV is generating as well
2. Reduced demand on the grid as the EV charging power is locally produced from PV [5]
3. Reduced cost of EV charging and reduced impact of changes in PV feed-in-tariffs [6]
4. The EV can be used as a storage for PV [7].

State of the art

The focus of this paper is on electric bikes (e-bikes) and how to sustainably charge them [8]–[10]. Currently, existing e-bike charging systems draw power from the AC grid, which results in indirect emissions at the electricity generation station [2]. To overcome this, solar e-bike charging stations have been built that typically make use of a solar inverter to feed PV power to the AC grid [11]. A standard e-bike power adapter connected to the AC grid is then used for e-bike charging. The disadvantage of such a design is the unnecessary power conversion from DC to AC and back, even though both the solar panels and e-bike battery operate on DC [12], [13]. Secondly, the lack of battery storage in these stations largely prevents them from being operated in off-grid mode or on days with very low insolation during the year. Finally, these stations do not integrate the physical design of the charging station with the electrical components which results in large electrical cabinets occupying space in the bike parking lot.

Contributions

This paper describes the development of a novel solar powered e-bike charging station that provides for sustainable charging of e-bikes, as shown in Fig. 1. The charging station has integrated storage and a bidirectional inverter that allows for both grid-connected and off-grid operation from a DC nanogrid. Besides the conventional AC charging of e-bikes via the e-bike power adapter, the charging station provides for direct DC charging of the e-bike from the DC power of the solar panels [14]. Third, contactless charging of e-bikes is possible by using inductive coils with magnets that are placed at the base of the charging station and on the kickstand of the e-bike. Finally, the physical structure of the charging station and the electrical design are cohesively integrated resulting in an environmentally integrated PV system (EIPV) design. The EIPV is designed for modularity, ergonomics, safety, and to withstand outdoor weather conditions

Solar e-bike charging station

Table I shows the specifications of the charging station and the key components. Eight Sunpower X20-327-BLK modules are used for the PV generation. They are connected in four parallel strings, with each string having two series connected panels. Fig. 2 shows the schematic of the electrical system. A maximum power point tracking (MPPT) converter (Victron BlueSolar 150/85) is used to extract power from the PV panels to charge the 48V lead-acid batteries [15]. The batteries, in turn, form a 48V DC nanogrid that is used for power exchange between all the components. An isolated DC-DC converter and a contactless charger based on a high-frequency DC/AC inverter are both connected to the 48V DC nanogrid for charging of e-bikes.

An inverter (Victron Multiplus 48/3000) feeds power from the 48V DC nanogrid to the single-phase AC grid [15]. The inverter has two AC outputs, one of which is connected to AC grid and the second which supports off-grid AC operation. The inverter is bidirectional and can be used for charging the battery from the grid for different grid operations such as peak shaving, energy arbitrage or emergency backup power. The charging station is sized in such a way that it can charge at least five e-bikes and a single e-scooter throughout the year, even under low winter insolation. A weather station records the incoming solar radiation, wind, and temperature for monitoring and research purposes [16].

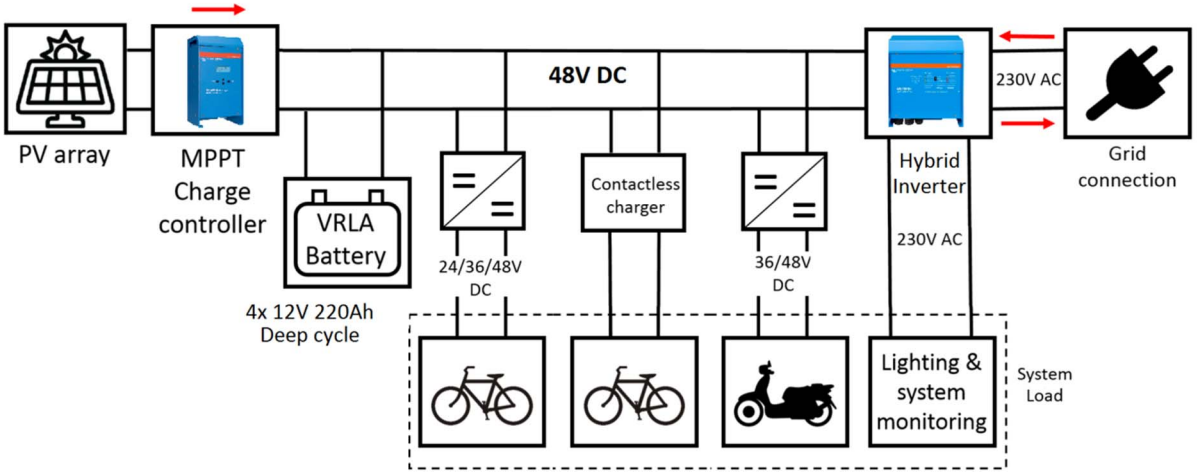

Fig. 2: Schematic of the solar e-bike station with 48V DC interconnection that facilities power exchange between the solar panels, e-bike chargers and the AC grid.

Table I: Specifications of the solar e-bike charging station

Solar panels	8x Sunpower X20-327-BLK, 327W
Battery	4x Victron Lead Acid Batteries, 220Ah, 12V
MPPT converter	Victron BlueSolar 150/85
Grid Inverter	Victron Multiplus 48/3000 Bidirectional
Weather station	Lufft WS503-UMB
Controller	Odroid C1+
AC connection	Three phase 400V 16A
e-bike Charging	1xAC, 4xDC (10-50V), 1x Contactless,

System Design

Fig. 3 shows a flowchart of the design process used to develop the e-bike station. The first three steps correspond to estimating the solar energy yield based on the weather parameters, PV panel orientation, and shading at the location. Then, the PV system is sized according to the e-bike charging demand. Next, the electrical design is done comprising of the power electronics converters for the PV, e-bikes, and AC grid. Then, the EIPV system design integrates all the components in a unified way. Finally, the system control and monitoring via the ODROID controller, weather station, and the website provides users with feedback and data for scientific research (http://solarpoweredbikes.tudelft.nl).

Charging demand

The first step in the system design is to estimate the e-bike charging demand (load). Table II shows the specifications of the e-bike and e-scooter that are considered for the system sizing [17]. The charging times indicated are based on the AC charger provided with the vehicle. Each e-bike battery has a capacity of 400Wh. A total of five such e-bikes, assuming that they arrive with completely drained batteries (the worst case), would translate to a load of 2000Wh. Similarly, for the e-scooter, the battery capacity is about 1920Wh. This means that the larger battery capacity of the e-scooter would require >12h charging time using a 100-150W charger. The system is designed to completely charge five e-bikes and one e-scooter daily, resulting in a total load of 3920Wh.

A base load of 90W is consumed by the lights, controller, display and the weather station. The base load consumption for a day translates to 2160 Wh. If the charging demand and baseload are combined, the net demand is approximately 6 kWh.

Local storage

The charging station has four 220Ah lead-acid gel batteries that provide a combined energy storage capacity of 10.5kWh. With 6kWh demand per day, it can provide close to two days of autonomy to the

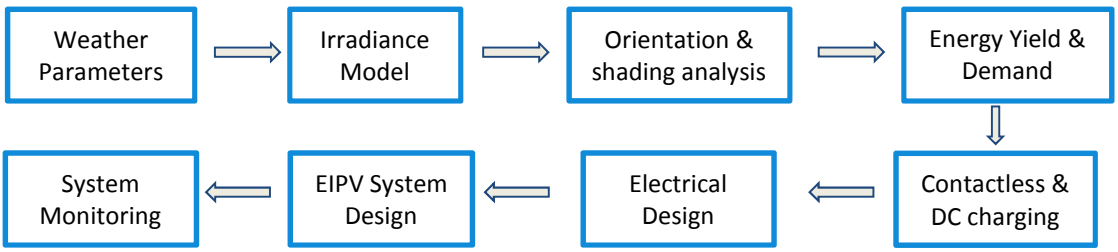

Fig. 3: Flowchart explaining the design of the e-bike charging station

Table II: Specifications of the E-bike and E-scooter

Model	E-bike	E-Scooter
	Batavus Trento E-go	**Novox C-50**
Type	Lithium-ion	Lithium-ion
Capacity (Wh)	400	1920
Current (Ah)	11	40
Voltage (V)	36	48
Nominal Range (km)	120	60-90
Normal charging time (h)	3.5	5
Fast charging time(h)	<2	2

system. The battery plays a crucial role in providing off-grid operation capability to the charging station. They are operated with a maximum depth of discharge of 90 %. Lead acid gel batteries were chosen due to the lower cost compared to lithium-ion batteries and much longer lifetime than standard lead-acid batteries. The solar MPPT converter allows the battery to be charged from the solar panels, which is the preferred (default) mode of charging the batteries. In case of insufficient solar generation, the bidirectional DC-AC grid inverter allows the battery to get charged and discharged from the grid.

Power balance

The power balance equation of the system is:

$$P_{PV} + P_{grid} = P_{batt} + P_{loss} + P_{load} \quad (1)$$

where P_{grid} is the power drawn from the grid, P_{PV} is the PV power, P_{batt} is the charging power of the battery, P_{loss} is the total energy conversion losses and P_{load} is the power consumption of the station including that of the e-bikes and the base load.

PV system design

The PV generation potential at the installation location is estimated based on the solar insolation, wind, temperature, panel orientation, and shading. The meteorological data used for the PV system modelling are acquired from the 2013 Cabauw Experimental Site for Atmospheric Research (CESAR) database, with a resolution of 1 min. Based on the meteorological data, the solar power generated from the PV system for different azimuth and orientation is estimated using [18]–[22] where G_{dir}, G_{diff}, G_{alb} are the direct, diffused and albedo irradiance incident on the module with a tilt β and azimuth A_m, G_{DNI} is the direct normal irradiance, G_{DNI} is the diffuse horizontal irradiance, θ_i is the angle of incidence of the direct irradiance beam on the panel, Φ is the absorptivity, h_c is the overall conductive heat transfer coefficient, $h_{r,sky}, h_{r,gr}$ are the radiative heat transfer coefficient to the sky, R is the reflectivity of the solar modules, η is the efficiency of the modules and $T_{amb}, T_{sky}, T_{gr}, T_{cell}$ are the ambient, sky, ground and PV cell temperature:

$$G_{dir(\beta,Am)} = G_{DNI}\, cos(\theta_i) \quad (2)$$

$$G_{diff(\beta)} = G_{DHI}\,(1 + cos\beta)/2 \quad (3)$$

$$G = G_{dir(\beta,Am)} + G_{diff(\beta)} + G_{alb} \quad (4)$$

$$T_{cell} = \frac{\Phi G + h_c T_{amb} + h_{r,sky} T_{sky} + h_{r,gr} T_{gr}}{h_c + h_{r,sky} + h_{r,gr}} \quad (5)$$

Here, the heat transfer coefficients are estimated using an iterative procedure, where $T_{sky} = 0.0522\, T_{amb}^{2/3}$. Based on the above equation the output power of the PV modules P_{PV} can be estimated:

$$P_{PV} = P_{STC}\left(\frac{G}{G_{STC}}\right)\{1 - \gamma(T_{cell} - 25)\} \quad (6)$$

where P_{STC} is the module power at Standard Test Conditions (STC), G_{STC} is the irradiance under STC and γ is the module temperature coefficient. For the Sunpower modules used, P_{STC}=327, G_{STC}=800W/m^2 and γ=-0.3 %/°C.

Shading analysis

Since the PV panels will be installed at the ground level and not on the rooftop of a building, shading from nearby buildings has a significant impact on the system output. In order to account for the shading at the installation location due to the adjacent buildings, a combination of hardware (Horicatcher) and software (Meteonorm) methods are used. The Horicatcher consists of a digital camera mounted above a horizon mirror as shown in Fig. 4(a). The device is placed in the location of the PV panels, and an image of the horizon is taken on the camera as shown in Fig. 4(b). The image is then processed using the associated Meteonorm software to estimate the PV output including the shading factor. The shading caused by the tall Electrical Faculty building in front of the bike station in the afternoon can be clearly seen in Fig. 4(b).

PV system yield and optimal orientation

Based on the meteorological and shading data, the annual yield of the PV system is estimated for different orientations. For the whole year, a tilt of 28° and azimuth facing south was found to result in maximum annual yield [5]. However, the motive was to ensure that there is sufficient generation in the month of December when there is the least solar insolation of the year. For the month of December, the optimal tilt for maximum monthly yield was 65°, as shown in Fig. 5(a). Conversely, when the tilt is increased from 28° to 65°, the annual yield is dramatically reduced by up to 20%. Hence, a trade-off is made to set the tilt angle at 51°, which results in <5% reduction in annual yield compared to 28° and 1% reduction in December yield compared to 65°.

Based on the charging demand, the PV system is sized to a rated power of 2.61 kW. The corresponding estimated annual energy yield is 1809 kWh/year providing an average daily yield of 4.95kWh/day as shown in Fig. 5(b). This means that >80% of the total load demand can be supplied by the PV system. At the same time, we have to keep in mind that there is about six times difference in energy yield between the winter and summer months in Fig. 5(b). That is why a grid connection is required so as to provide the energy demand in winter. While the battery cannot provide seasonal storage, it can facilitate off-grid operation and help manage the diurnal solar insolation variation.

Power electronic converters for chargers

Two types of e-bike charging were developed for the charging station: DC charging and a contactless charging. The aim of the DC charging is to provide a DC cable that users can connect directly to the battery of their e-bike and charge it. This negates the need for an AC power adapter providing convenience to the user and preventing any theft of the adapter. In case of the contactless charging, the motive is to increase the user convenience further by removing all charging cables [23], [24].

DC charging system

Fig. 6(a) shows the topology and of the interleaved flyback DC-DC isolated converter used for the DC charger that works off the 48V nanogrid. This converter was obtained from Involar [25]. The charger detects the voltage of the e-bike battery (12-48V) and accordingly adjusts its output voltage for charging. Fig. 6(b) shows the realization of the flyback converter. One of the challenges with the DC charging is to mimic any communication that exists between the e-bike AC power adapter and the e-bike battery. Without this communication, the charging process does not start. The DC charging has

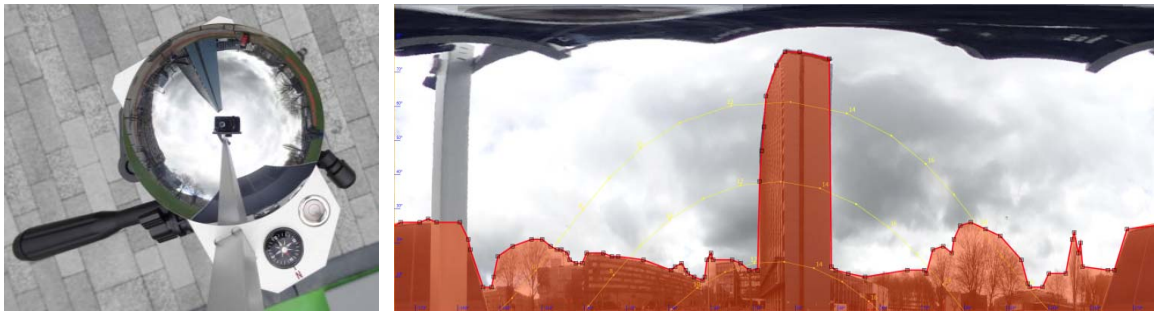

(a) (b)

Fig. 4: (a) The Meteonorm Horicatcher is used to estimate the (b) shading due to nearby buildings at the location of the e-bike charging station

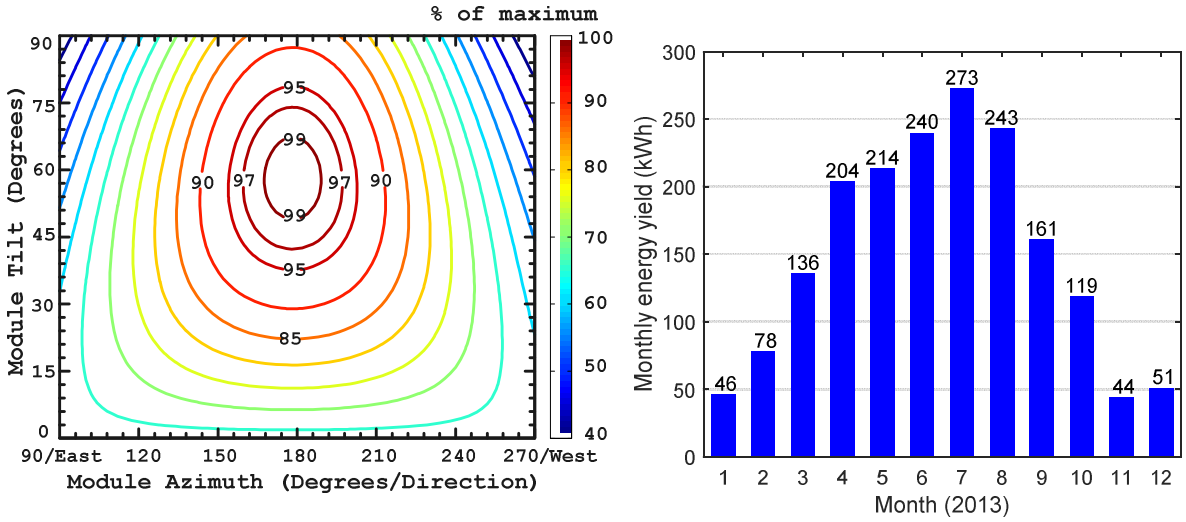

(a) (b)

Fig. 5: (a) PV system yield (% of maximum) for different orientations considering December month (b) Estimated monthly energy yield of 2.6kW PV system tilted at 51° and facing south

been tested with Gazelle and Batavus e-bikes at TU Delft, and testing of e-bikes from other brands is currently underway.

Contactless charging system

Fig. 7 shows the schematic of the contactless power transfer system for the e-bike. The contactless charging system directly derives its power from the 48V DC nanogrid. The charger consists of mainly two components: the power flow control circuit enclosed by the purple enclosed area and the contactless power transfer circuit, indicated by the red dashed enclosed area. The power flow control circuit is a DC-DC buck converter, and the amount of power to be wirelessly transferred can be controlled and/or shut down using it.

On the other hand, the contactless power transfer circuit is built around a series-series resonant inductive circuit, with a passive load. On the primary side, there is a full bridge MOSFET inverter operated with a controlled frequency. This frequency is adjusted based on the power transfer to ensure power exchange at optimum efficiency. The bipolar PWM modulator is operated at this optimum frequency and it, in turn, controls the MOSFETs in the inverter. The amount of transferred power is measured using a current sensor placed between the DC-DC power flow control circuit and the high-frequency inverter. The developed primary side PCB is shown in Fig. 8(a).

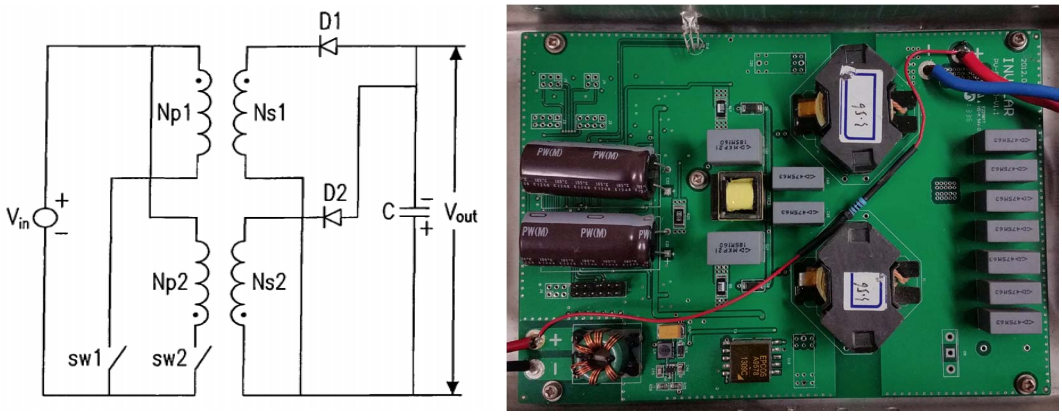

(a) (b)

Fig. 6: (a) Interleaved flyback topology of the DC e-bike charger (b) PCB of the DC charger

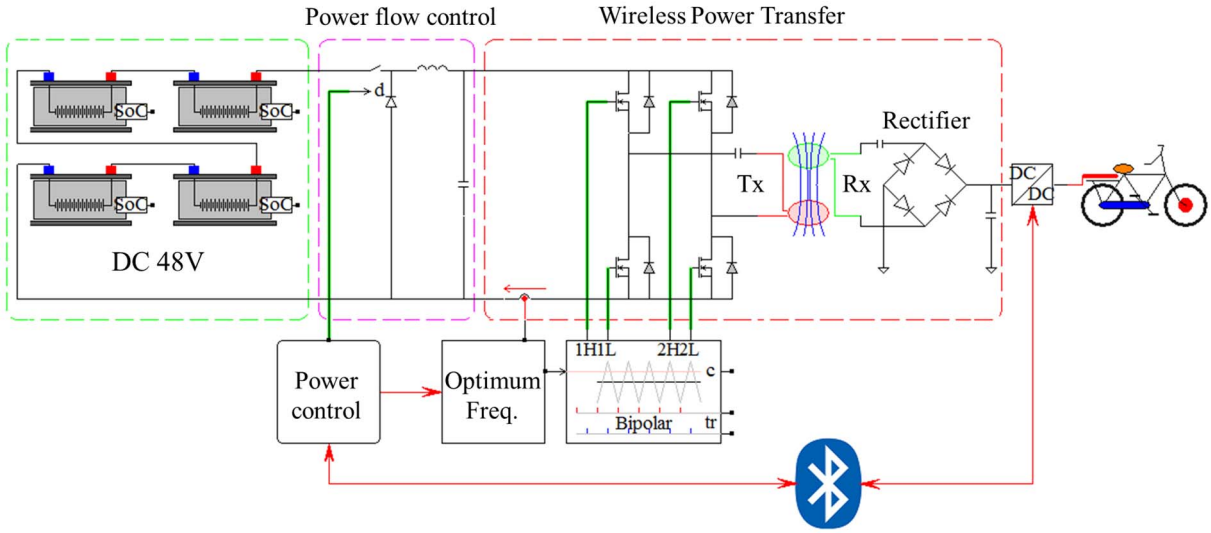

Fig. 7: Schematic of the contactless power transfer system for the e-bike

The primary side coil (TX) is connected to the inverter together with a series capacitor for compensation. This primary side coil is placed underneath the charging station. The primary and secondary coil exchange power via the principle of electromagnetic induction. The secondary coil is placed on the kickstand of the e-bike as shown in Fig. 8(b). The secondary coil (RX) is connected via the series compensation capacitors to a diode rectifier bridge. The rectified power pulses are filtered by a capacitor. The battery management system of the e-bike is directly connected to the output of the diode bridge. In this way, the battery charging is controlled by its own battery management system being part of the e-bike battery pack. Protection circuitry (not shown in the figure) takes care that the output voltage is limited to a maximum value.

E-bike and foreign object identification

The object detection circuit identifies if an object is placed on top of the charging pad. As soon as an object is detected, the power transfer is started from the primary side, and the communication via Bluetooth becomes active. For example, when placing the e-bike over the charging pad, the secondary coil is powered and thereby allows the start-up of the DC-DC converter on the secondary side. This will, in turn, start communication via Bluetooth from the secondary side with the primary side control. Thus, receiving correct information from the secondary side allows the primary side to sustain the power transfer. In case of a foreign object, there is no communication from the secondary side, and the power transfer from the primary side is shut down. Subsequently, if the e-bike is removed after charging, this will cut-off the power to the secondary coil and hence will stop the communication

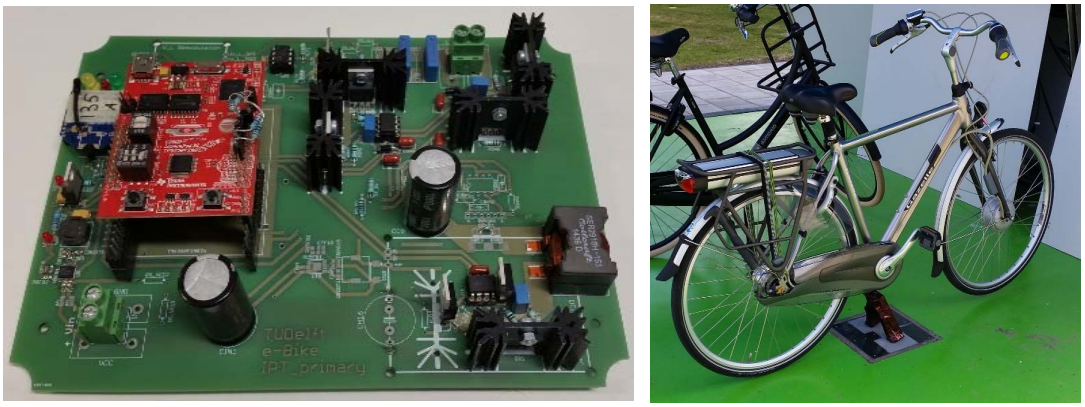

(a) (b)

Fig. 8: (a) Primary side PCB with the power flow control circuit and inverter (b) e-bike with primary coil placed underneath the station and secondary coil built onto the kickstand

(a) (b)

Fig. 9: (a) Inverter, MPPT tracker, protection and monitoring circuit (b) DC-DC converter and protection for DC charging of e-bike

via Bluetooth. As soon as the communication terminates, the primary side control will stop the power transfer from the primary coil.

Experimental realization

Environment Integrated PV system

All the components of the solar charging station are combined together to form an Environment Integrated PV system (EIPV) built on the university campus as shown in Fig. 1. The benefit is that all mechanical and electrical components are integrated together resulting in a single structure that combines aesthetics, modularity, safety, ergonomics, and usability. The high-efficiency Sunpower X20-327-BLK modules with a relatively high €/W_p are used in this EIPV as this reduces the total area occupied by the PV system. In return, this drastically reduces the amount of steel required for the station structure which has a relatively higher cost for both material and labor.

Fig. 9(a) shows the solar MPPT converter, bidirectional inverter, grid islanding device, control and protection circuity for both the devices. Fig. 9(b) shows the DC-DC converters for the e-bike DC charging, charging measurement circuit and the ODROID central controller that is responsible for communicating with all the devices. The ODROID also reads data from all devices like the VICTRON system and weather station and logs them centrally into an internet server [26].

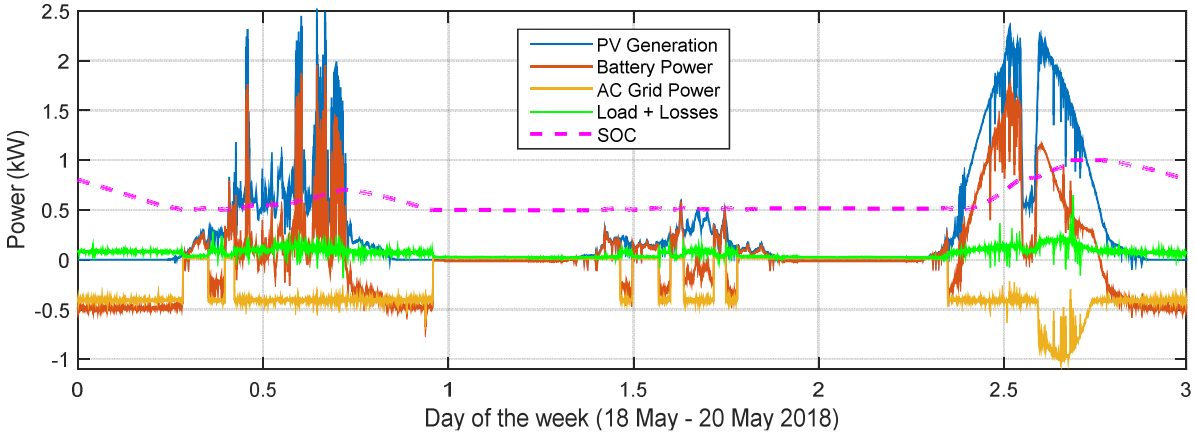

Fig. 10: Measurement of the PV, battery and grid power over one week (a) in summer (b) in winter

Power measurement

The PV power, grid power, battery power and SOC, and the load power are measured and logged continuously. The seasonal variation in the solar generation has a significant impact on the system, with the measured daily energy yield varying up to 25 times, from 0.64 kWh/day to 15.4 kWh/day. Different power management strategies can be used for controlling the battery (dis)charging from the PV and grid. One such strategy that has been implemented now is as follows: the station provides the e-bike charging load and base load; and constantly feeds at least 400W to the AC grid when either the battery SOC >50% or if there is an excess solar generation.

To further demonstrate the operation, the output power of the system for three consecutive days (May 18 to 20) is shown in Fig. 10 with a yield of 8.17kWh, 3.03kWh, and 15.22 kWh, respectively. First, it can be seen on the sunny Day 3 that the solar power is used to supply the load, feed 400W to the AC grid and to charge the battery from 50% to 100% state of charge (SOC). Second, the dip in the PV generation in the afternoon on Day 3 due to shading from the faculty building can be clearly observed. Third, when the solar generation is low/ zero (in the night and during the day on Day 1 and 2), the battery is discharged to feed power to the AC grid, as long as the SOC>50%. Finally, when is neither sufficient solar generation nor the battery SOC>50%, no power is fed to the AC grid.

Conclusions

The paper describes the development of a novel charging station for e-bikes and scooters that is powered from solar panels. The station offers AC, DC and contactless charging options from 2.6kW PV system. It has an integrated storage of 10.5kWh that can support both grid connected and off-grid operation via a bidirectional inverter powered from a DC nanogrid. The system can be monitored and controlled remotely using an ODROID controller that also helps in maintaining communication between the various components. The environmentally integrated PV system combines all the mechanical, civil and electrical components in a single structure that cohesively integrates aesthetics, modularity, safety, ergonomics, and convenience.

References

[1] D. P. Birnie, “Solar-to-vehicle (S2V) systems for powering commuters of the future,” *J. Power Sources*, vol. 186, no. 2, pp. 539–542, Jan. 2009.

[2] M. Messagie, F.-S. S. Boureima, T. Coosemans, C. Macharis, and J. Van Mierlo, “A range-based vehicle life cycle assessment incorporating variability in the environmental assessment of different vehicle technologies and fuels,” *Energies*, vol. 7, no. 3, pp. 1467–1482, Mar. 2014.

[3] C. Hamilton *et al.*, “System architecture of a modular direct-DC PV charging station for plug-in electric vehicles,” in *Annual Conference on IEEE Industrial Electronics Society*, 2010, pp. 2516–2520.

[4] G. Carli and S. S. Williamson, “Technical Considerations on Power Conversion for Electric and Plug-in Hybrid Electric Vehicle Battery Charging in Photovoltaic Installations,” *IEEE Trans. Power Electron.*, vol.

28, no. 12, pp. 5784–5792, Dec. 2013.
[5] G. R. Chandra Mouli, P. Bauer, and M. Zeman, “System design for a solar powered electric vehicle charging station for workplaces,” *Appl. Energy*, vol. 168, pp. 434–443, Apr. 2016.
[6] G. R. Chandra Mouli *et al.*, “Economic and CO2 Emission Benefits of a Solar Powered Electric Vehicle Charging Station for Workplaces in the Netherlands,” in *IEEE Transportation Electrification Conference and Expo (ITEC)*, 2016, pp. 1–7.
[7] G. R. Chandra Mouli, J. H. Schijffelen, M. van den Heuvel, M. Kardolus, and P. Bauer, “A 10kW Solar-Powered Bidirectional EV Charger Compatible with Chademo and COMBO,” *IEEE Trans. Power Electron.*, 2018.
[8] Cheng-Hu Chen and Ming-Yang Cheng, “Implementation of a Highly Reliable Hybrid Electric Scooter Drive,” *IEEE Trans. Ind. Electron.*, vol. 54, no. 5, pp. 2462–2473, Oct. 2007.
[9] F. Pellitteri, V. Boscaino, A. O. Di Tommaso, F. Genduso, and R. Miceli, “E-bike battery charging: Methods and circuits,” in *2013 International Conference on Clean Electrical Power (ICCEP)*, 2013, pp. 107–114.
[10] P. Fairley, “China’s cyclists take charge: electric bicycles are selling by the millions despite efforts to ban them,” *IEEE Spectr.*, vol. 42, no. 6, pp. 54–59, Jun. 2005.
[11] S. Mesentean, W. Feucht, A. Mittnacht, and H. Frank, “Scheduling Methods for Smart Charging of Electric Bikes from a Grid-Connected Photovoltaic-System,” in *2011 UKSim 5th European Symposium on Computer Modeling and Simulation*, 2011, pp. 299–304.
[12] G. R. Chandra Mouli, P. Bauer, and M. Zeman, “Comparison of system architecture and converter topology for a solar powered electric vehicle charging station,” in *International Conference on Power Electronics and ECCE Asia (ICPE-ECCE Asia)*, 2015, pp. 1908–1915.
[13] V. Vega-Garita, L. Ramirez-Elizondo, G. R. C. Mouli, and P. Bauer, “Review of residential PV-storage architectures,” *2016 IEEE Int. Energy Conf.*, pp. 1–6, 2016.
[14] L. Mackay, T. G. Hailu, G. R. Chandra Mouli, L. Ramirez-Elizondo, J. A. Ferreira, and P. Bauer, “From DC Nano- and Microgrids Towards the Universal DC Distribution System – A Plea to Think Further Into the Future,” in *2015 IEEE Power & Energy Society General Meeting*, 2015, pp. 1–5.
[15] Victron Energy, “MultiPlus 48/3000/35-16 & BlueSolar Charger MPPT 150/85.”
[16] Lufft, “WS503-UMB Smart Weather Sensor (https://www.lufft.com).”
[17] D. C.-H. Chao, P. J. van Duijsen, J. J. Hwang, and C.-W. Liao, “Modeling of a Taiwan fuel cell powered scooter,” in *2009 International Conference on Power Electronics and Drive Systems (PEDS)*, 2009, pp. 913–919.
[18] M. Paulescu, E. Paulescu, P. Gravila, and V. Badescu, “Weather Modeling and Forecasting of PV Systems Operation,” *Green Energy Technol.*, vol. 103, 2013.
[19] J. E. Braun and J. C. Mitchell, “Solar geometry for fixed and tracking surfaces,” *Sol. Energy*, vol. 31, no. 5, pp. 439–444, 1983.
[20] I. Reda and A. Andreas, “Solar position algorithm for solar radiation applications,” *Sol. energy*, 2004.
[21] A. Q. Jakhrani, A. K. Othman, A. R. H. Rigitand, and S. R. Samo, “Comparison of solar photovoltaic module temperature models,” *World Appl. Sci. J.*, vol. 14, pp. 1–8, 2011.
[22] O. Isabella *et al.*, “Comprehensive modelling and sizing of PV systems from location to load,” *MRS Proc.*, vol. 1771, pp. 1–7, Apr. 2015.
[23] D. Iannuzzi, L. Rubino, L. P. Di Noia, G. Rubino, and P. Marino, “Resonant inductive power transfer for an E-bike charging station,” *Electr. Power Syst. Res.*, 2016.
[24] F. Pellitteri, G. Ala, M. Caruso, S. Ganci, and R. Miceli, “Physiological compatibility of wireless chargers for electric bicycles,” in *2015 International Conference on Renewable Energy Research and Applications (ICRERA)*, 2015, pp. 1354–1359.
[25] Involar Micro-inverters, “http://www.involar.eu/.”
[26] TU Delft solar e-bike charging station, “http://solarpoweredbikes.tudelft.nl.”